

AGING METALLURGY AND MECHANICAL PRPERTIES ON Al-Si-Cu-Mg DIE CASTING ALLOY

*T. Ando¹, S. Onuki¹, R. Enomoto¹, M. Tejima², and Y. Okada²

¹*Muroran Institute of Technology
Muroran, Hokkaido, Japan*

(*Corresponding author: ando@mmm.muroran-it.ac.jp)

²*Toyota Motor Corporation
Toyota, Aichi, Japan*

ABSTRACT

Al-Si-Cu-Mg die casting alloys are widely used in the automotive industry, and recent advancements in high pressure die casting technology enable heat treating products to achieve desirable properties. However, CO₂ emissions associated with die-casting production lines should be reduced to address the global warming issue. In this study, the relation between the microstructures and thermal stability of precipitates formed during isothermal aging at 423, 485, and 558 K of Al-11.0 mass%Si-1.8 mass%Cu-0.2 mass%Mg (JIS ADC12) was investigated using Vickers hardness tests and transmission electron microscopy (TEM). The hardness tests and TEM results showed that Si compounds and Al-Cu compounds enhanced the mechanical properties of the alloy and that the predominant compound affecting the mechanical properties differed between specimens treated at 423 K and those treated at 558 K. Moreover, additional aging at 423–458 K resulted in a material with a Vickers hardness higher than that of the isothermally single-aged material. Differential scanning calorimetry, differential elemental analysis, and selected-area diffraction analysis using TEM suggested that the combination of Al-Cu compounds precipitated at low aging temperatures and Si compounds precipitated during preliminary aging increased the mechanical strength, resulting in a maximum hardness of 130 HV.

KEYWORDS

Al-Si-Cu-Mg alloy, Artificial aging, Automotive industries, Die casting, Precipitates

INTRODUCTION

Al–Si–Cu–Mg die casting alloys have well-balanced mechanical properties, machinability, and castability. These alloys are therefore widely used in the automotive industry because of their superior characteristics, accounting for >90% of the aluminum used in die casting production. As a substitute for iron-based materials, these alloys have contributed to the development of lightweight vehicles.

Dong et al. (2014) reported that the heat treatment of die casting materials is effective for changing their dimensions under high temperatures as a result of the precipitation of solid-solution elements. Recent advancements in high pressure die casting technology have led to the application of heat treatments of Al–Si–Cu–Mg alloy products to reduce fuel consumption and satisfy customer needs. Although attempts to reduce CO₂ emissions have focused on fuel consumption in cars and fuel efficiency regulations have become increasingly strict in recent years, CO₂ discharged from production lines should also be reduced without adversely affecting the properties of the product. Heat treatments for artificial aging after solution treatment (T6 treatment) and after casting (T5 treatment) are CO₂ discharge sources, which together with a holding furnace account for >80 % of the CO₂ discharged during the casting process.

Although a few studies on the aging of die casting aluminum alloys have been reported, the mechanism of hardening during the T5 treatment of an actual die-cast material remains unclear because previously reported results are inconsistent. Nonetheless, the properties and metallurgies of aged aluminum casting materials have been studied. Mishra et al. (2001) reported that the S' phase formed first and was then partially dissolved as Si formed in an Al–Si–Cu–Mg alloy prepared via direct-quenched casting. In other study, a T5-treated Al–Si–Mg–Mn die-casting alloy was reported to exhibit hardening (Yamagata & Kitsunai, 2006). Inoue et al. (2011) reported that pre-aging showed the positive effect on the precipitation behaviour of Al–Si–Mg alloy during artificial aging. In contrast, an investigation of precipitation in Al–Si–Cu–Mg alloys for die casting showed that precipitation-hardening did not occur in the T5-treated material but did occur in the T6-treated material, wherein the strengthening was caused by precipitation of the S'' phase (Konno et al., 2016).

In this study, we investigated the relation between the microstructures and thermal stability of precipitates formed during isothermal artificial aging following die casting, with the objective of controlling the mechanical properties via a low-energy heat treatment. The effect of two-step artificial aging to control the mechanical properties of the alloy was also investigated.

EXPERIMENTAL

The samples were cut from an actual die casting block cylinder using a 2000-ton-class high pressure die casting machine. The chemical composition of the samples was Al-11.0 mass%Si-1.8 mass%Cu-0.2 mass%Mg (JIS ADC12). Heat treatments were performed using an oil bath for short-term treatments (<3.6 ks) and an electric furnace for long-term treatments (>18 ks) at 423, 493, and 563 K to investigate the effects of isothermal artificial aging on the alloy's properties. Furthermore, additional aging experiments at 423 K for 86 ks–0.6 Ms were performed after a preliminary aging treatment for 600 s at 443–563 K to investigate the effect of two-step artificial aging. The temperature difference between the oil bath and electric furnace was corrected using a K-type thermocouple.

The changes in the mechanical properties of the samples were investigated using Vickers hardness measurements. A Future-tech FV-300A test apparatus was used under conditions of a 4.9-N load applied for 6 s. The average value of five measured points was adopted as the hardness.

The observations to investigate precipitates were performed using transmission electron microscopy (TEM). A JEOL JEM-2100F transmission electron microscope was operated at an acceleration voltage of 200 kV. TEM samples were prepared using Struers jet polishing equipment with an electrolyte composed of 30% nitric acid in methanol. Scanning transmission electron microscopy (STEM) was used to observe the morphology of the precipitates; the precipitates' composition and structure were analyzed via

energy-dispersive X-ray spectrometry (EDS) and selected-area diffraction (SAD), respectively.

Differential scanning calorimetry (DSC) analysis was performed on a Hitachi DSC-7000X. Samples were subjected to a heating rate at 0.17 K/s from 353 to 600 K. The analysis was initiated at 353 K because of the restriction of the Guinier–Preston zone formed at approximately 300 K (Ikeno et al., 2001).

RESULTS AND DISCUSSION

Figure 1 shows Vickers hardness curves versus aging time of samples aged at 423, 488, and 558 K. Age-softening is observed for all of the aged samples at the first stage, followed by age-hardening, where the time required to reach peak hardness tended to be longer and the peak hardness tended to increase with decreasing aging temperature. The peak hardness after age-softening of the as-cast sample, which was in a state of recovery. The age-softening was caused by the annihilation of dislocations (Zhu & Starink, 2008), which were deduced to have been introduced during the preliminary manufacturing process in this case. However, remarkable hardening occurred after the aging at 423 K; the peak hardness value was 125 HV, which is substantially higher compared with the hardness values of the samples aged at 488 and 558 K.

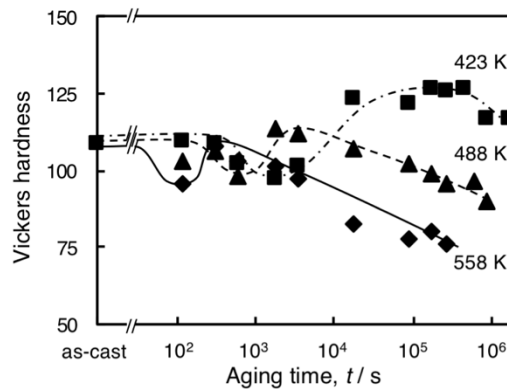


Figure 1. Effects of aging temperature on the Vickers hardness curves of die cast Al–Si–Cu–Mg alloy

Figure 2 shows a TEM image of a sample in the as-cast state. The EDS maps show silicon and copper dispersed homogeneously in the aluminum matrix. The SAD pattern, which was acquired on the aluminum $\langle 100 \rangle$ zone axis, shows that the as-cast material was a supersaturated solid solution.

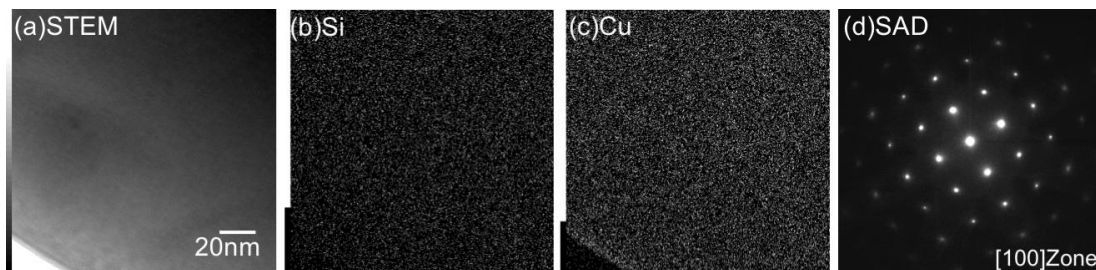


Figure 2. TEM images and corresponding diffraction pattern of as-cast Al–Si–Cu–Mg alloy: (a) STEM image, (b) EDS map of silicon, (c) EDS map of copper, and (d) SAD pattern of $[100]_{Al}$

Figures 3 and 4 show the TEM images of samples aged at 558 K for 600 s and at 423 K for 260 ks. Rod-shaped and circular-shaped precipitates were confirmed in the samples aged at 558 and 423 K, respectively. The precipitates formed during aging at 558 K were β' phase (Cayron & Buffat, 2000) silicon compounds, as indicated by the EDS map and SAD analysis on the aluminum $\langle 100 \rangle$ zone axis (see Figure

3). However, the EDS map in Figure 4 shows that the precipitates formed during aging at 423 K exhibited a high copper concentration at the same position of the precipitates. Notably, the SAD spots of the precipitates could not be identified because of difficulty associated with inclining a thin foil to a metallurgical low-index-incident-beam direction.

The silicon-compound precipitates were observed only in the sample aged at 558 K. This observation is attributed to either insufficient copper diffusion or inadequate reaction time, or both, for the formation of the β' phase, as shown in Figure 3. Therefore, copper compounds formed during prolonged aging at 558 K and further strengthened the alloy. Because of their large size, the β' precipitates could not contribute to the reinforcement of the alloy. This behaviour is clearly related to the peak hardness in the state of recovery on the hardness curve. We concluded that the specimens artificially aged at 558 and 488 K, which exhibited the same hardness as the as-cast sample, were overaged. Therefore, the combination of a preliminary short-term artificial aging treatment, which formed β' precipitates, and a secondary artificial aging at 423 K, which formed copper compounds, led to the higher hardness of the Al–Si–Cu–Mg die casting alloy. In previous studies (Konno et al., 2016), a lath-shaped S'' phase that precipitated during T6 treatment was found to strengthen an Al–Si–Cu–Mg die casting alloy, whereas the pre- S'' phase with a disk shape and without a crystal structure exerted no strengthening effect. However, disk-shaped precipitates were observed in the strengthened samples in this study. We concluded that clarifying the relation between microstructures and precipitation-hardening is crucial.

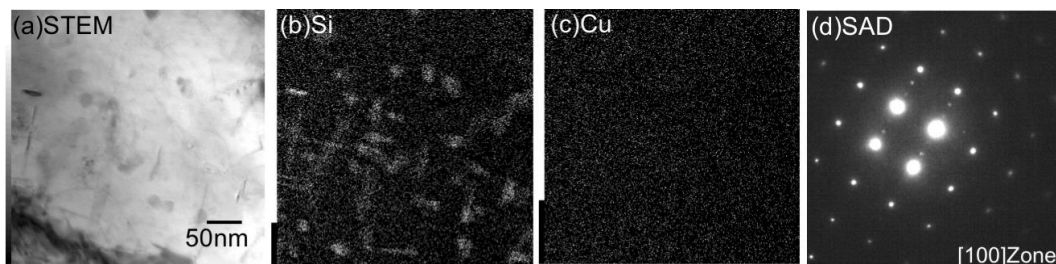


Figure 3. TEM image and corresponding diffraction patterns of die casting Al–Si–Cu–Mg alloy aged at 558 K for 600 s: (a) STEM image, (b) EDS map of silicon, (c) EDS map of copper, and (d) SAD pattern of $[100]_{Al}$; small spots correspond to β' precipitates

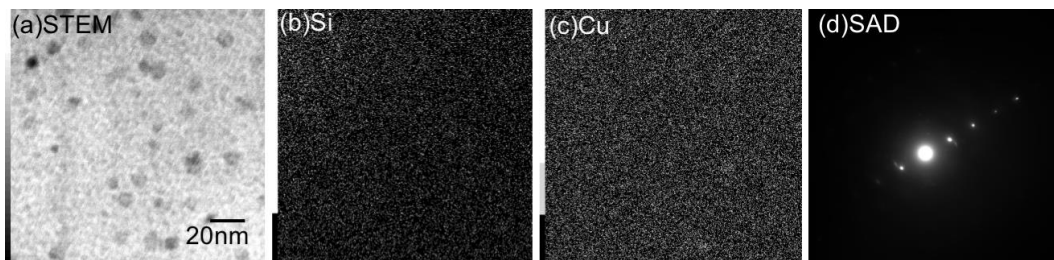


Figure 4. TEM image and corresponding diffraction pattern of die casting Al–Si–Cu–Mg alloy aged at 423 K for 260 ks: (a) STEM image, (b) EDS map of silicon, (c) EDS map of copper, and (d) SAD pattern; small spots correspond to precipitates

Figure 5 shows the dependence of the Vickers hardness on the secondary aging time. The secondary aging temperature was 423 K for the sample preliminarily aged for 600 s at 443–533 K. The aging time of 600 s was based on the results in Figure 1, which show a change in hardness. Samples aged at 443 and 458 K softened during the aging at 600 s, and the other samples exhibited the same hardness as the as-cast sample (Figure 1). These results indicate that 600 s as the preliminary aging time could be reasonably assumed to be the critical aging time at 443 and 458 K for the Al–Si–Cu–Mg die casting alloy because the peak hardness of samples aged at temperatures >473 K could not exceed that achieved for the

sample aged at 423 K. The hardness of the samples preliminarily aged at 443 and 458 K was 125 HV, which was the maximum hardness attained via isothermal aging at 423 K for approximately 100 ks, and the peak hardness was >125 HV. In particular, the highest hardness of 130 HV was achieved using a combination of preliminary and secondary aging temperatures of 458 and 423 K, respectively.

Figure 6 shows the DSC thermogram of the as-cast material aged at 458 K for 600 s, the sample preliminarily aged at 458 K for 600 s and secondarily aged at 423 K for 173 ks, and the sample aged at 423 K for 260 ks. An exothermic peak was observed at approximately 520 K (labelled as A) in the thermograms of both the as-cast sample and the sample aged at 458 K for 600 s. These exothermic processes are assumed to represent the formation of the β'' phase (Ikeno et al., 2001), and the aging of the as-cast sample decreased the exothermic heat volume. The preliminary aging at 458 K accelerated the formation of the β'' phase in the samples. By contrast, the endothermic peaks at approximately 490 K (labelled as B), as shown in Figure 6(c) and (d), are associated with the formation of clusters and with dissolution of the S'' phase (Wang et al., 2006).

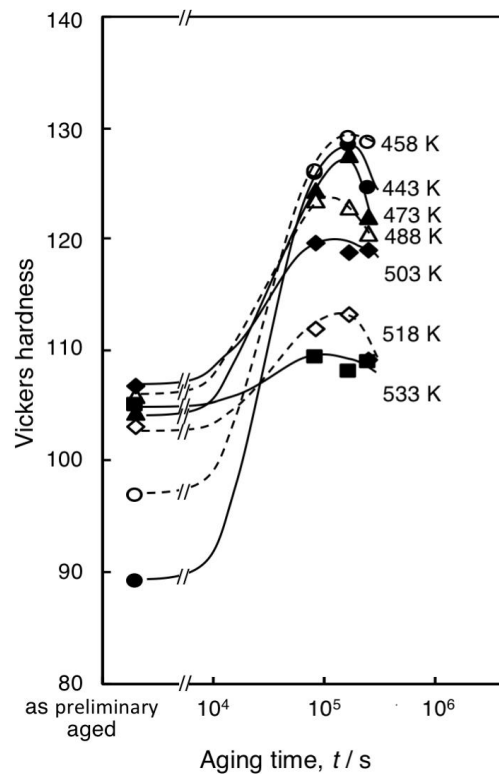


Figure 5. Effects of the preliminary aging temperature on the Vickers hardness curves of die cast Al-Si-Cu-Mg alloy for specimens subjected to secondary aging at 423 K (each temperature in the figure represents the temperature of preliminary aging)

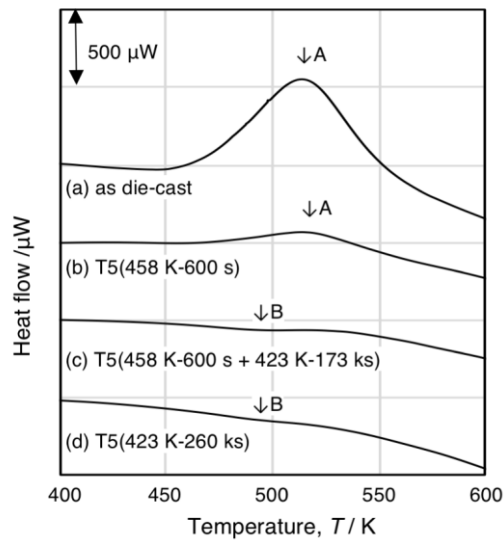


Figure 6. DSC thermograms of die casting Al-Si-Cu-Mg alloy: (a) as die-cast, (b) as aged at 458 K for 600 s, (c) as preliminarily aged at 458 K for 600 s and secondarily aged at 423 K for 173 ks, and (d) as aged at 423 K for 260 ks

Figure 7 shows the TEM images and corresponding diffraction pattern of die casting Al-Si-Cu-Mg alloy aged at 458 K for 600 s. Silicon and copper were not concentrated in the aluminum matrix in Figures 7(b) and 7(c). However, SAD analysis of the aluminum $\langle 110 \rangle$ zone axis indicated the existence of small spots corresponding to the β'' phase in the aluminum matrix. This observation is in good agreement with the decrease in intensity of the exothermic peak at approximately 520 K in the thermogram of the sample aged at 458 K for 600 s. Figure 8 shows a TEM image of the die casting Al-Si-Cu-Mg alloy preliminarily aged at 458 K for 600 s and secondarily aged at 423 K for 173 ks. Similar to the results in Figure 7, silicon and copper were not observed to be concentrated in the aluminum matrix in Figures 8(b) and 8(c). SAD analysis shows diffraction spots in disagreement with the presence of the β'' phase or β' phase. Figure 9 shows the diffraction spots and TEM images of the corresponding precipitates. Precipitates were approximately 20 nm in size, and the alignment of the diffraction spots indicates ordering. Precipitates in the Al-Si-Cu-Mg alloy have been reported to include coherent β'' and/or θ'' , S'' , Q'' , and Ω phases; however, none of these phases are consistent with the diffraction spots in Figure 9(b). To investigate the features of these precipitations in detail, we clarified the mechanism of precipitation strengthening of the die casting Al-Si-Cu-Mg alloy. Finally, although precipitates subjected to secondary aging at 423 K could not be identified, β'' and undefined precipitates, which were deduced to be copper compounds via TEM and DSC, were found to contribute to the reinforcement of the die casting Al-Si-Cu-Mg alloy.

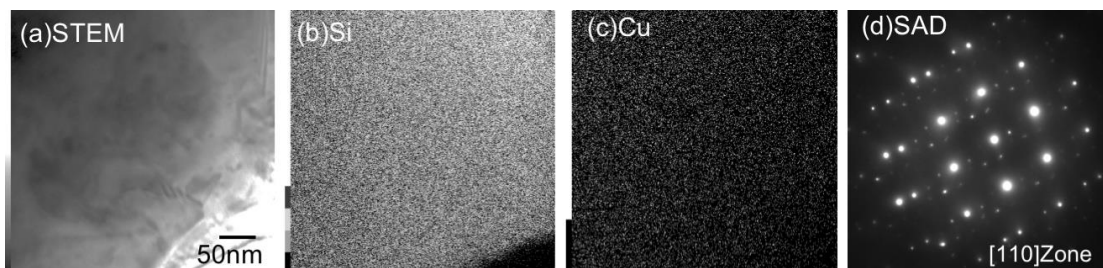


Figure 7. TEM images and the corresponding diffraction pattern of die casting Al-Si-Cu-Mg alloy aged at 458 K for 600 s: (a) STEM image, (b) EDS map of silicon, (c) EDS map of copper, and (d) SAD pattern of $[110]_{Al}$; small spots correspond to β'' precipitates

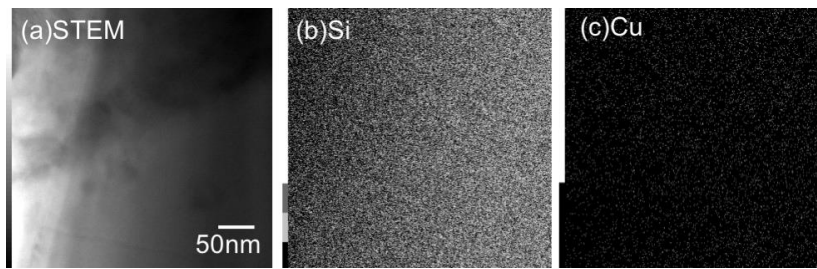


Figure 8. TEM images of die casting Al-Si-Cu-Mg alloy preliminarily aged at 458 K of 600 s and secondarily aged at 423 K for 173 ks: (a) STEM image, (b) EDS map of silicon, and (c) EDS map of copper

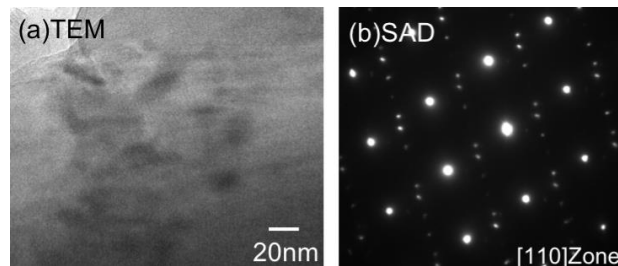


Figure 9. TEM image and corresponding diffraction pattern of die casting Al-Si-Cu-Mg alloy preliminarily aged at 458 K for 600 s and secondarily aged at 423 K for 173 ks: (a) TEM image and (b) SAD pattern of $[110]_{Al}$; small spots correspond to undefined precipitates

CONCLUSIONS

We clarified that the die casting alloy exhibited age-hardening when subjected to the T5 treatment. The precipitates of the die casting alloy controlling the hardness were the β' phase, β'' phase, and Al-Cu compounds. The combination of various precipitates yielded an alloy with good mechanical properties via low-energy heat treatment. The material secondarily aged at 423 K after preliminary aging at either 443 K or 458 K achieved a hardness of 125 HV with a shorter heating time, and its peak hardness was higher than that of the specimen isothermally aged at 423 K. In particular, the highest hardness of 130 HV was exhibited by the material that was preliminarily aged at 458 K.

REFERENCES

- Cayron, C., & Buffat, P. A. (2000). Transmission electron microscopy study of the β' -phase (Al-Mg-Si alloys) and QC phase (Al-Cu-Mg-Si alloys): Ordering mechanism and crystallographic structure. *Acta Materialia*, 48(10), 2639–2653. [https://doi.org/10.1016/S1359-6454\(00\)00057-4](https://doi.org/10.1016/S1359-6454(00)00057-4)
- Dong, S., Iwata, Y., Sugiyama, Y., & Iwahori, H. (2014). *Reports of the JFS Meeting*, 165, 92.
- Ikeno, S., Matsui, H., Matsuda, K., Terayama, K., & Uetani, Y. (2001). DSC measurement and HRTEM observation of precipitates in an Al-1.6 mass Mg₂Si alloy. *Japan Institute of Metals, Journal*, 65(5), 404–408. https://doi.org/10.2320/jinstmet1952.65.5_404
- Inoue, T., Goto, M., Yamaguchi, A., Otake, T., Kuroda, A., & Yoshida, M. (2011). Effect of pre-aging conditions on T5 heat treatment behavior of Al-9%Si-0.3%Mg die-casting alloy. *Keikin-zoku/Journal of Japan Institute of Light Metals*, 61(10), 507–512. <https://doi.org/10.2464/jilm.61.507>

- Konno, T. J., Sasaki, S., & Hamaoka, T. (2016). Transmission electron microscopic observation of precipitates in age-hardening die-cast aluminum alloys. *Journal of the Japan Institute of Light Metals*, 66, 291–297. <https://doi.org/10.2464/jilm.66.291>
- Mishra, R. K., Smith, G. W., Baxter, W. J., Sachdev, A. K., & Franetovic, V. (2001). The sequence of precipitation in 339 aluminum castings. *Journal of Materials Science*, 36(2), 461–468. <https://doi.org/10.1023/A:1004888831537>
- Wang, S.C., Starink, M.J., & Gao, N. (2006). Precipitation hardening in Al–Cu–Mg alloys revisited. *Scripta Materialia*, 54(2), 287–291. <https://doi.org/10.1016/j.scriptamat.2005.09.010>
- Yamagata, H. & Kitsunai, T. (2006). Strength improvement of high-quality die-casting part by T5 heat-treatment. 2006 Japan Die Casting Congress Transactions, 237–246.
- Zhu, Z. & Starink, M.J. (2008). Age hardening and softening in cold-rolled Al–Mg–Mn alloys with up to 0.4 wt% Cu. *Materials Science and Engineering: A*, 489(1–2), 138–149. <https://doi.org/10.1016/j.msea.2007.12.019>